Specialized pro-resolving lipid mediators inhibit the priming and activation of the macrophage NLRP3 inflammasome

Aritz Lopategi[*], Roger Flores-Costa[*], Bibiana Rius[*], Cristina López-Vicario[*,†], José Alcaraz-Quiles[*], Esther Titos[*,†,‡] and Joan Clària[*,†,‡,§]

[*]Department of Biochemistry and Molecular Genetics, Hospital Clínic-IDIBAPS; [†]Centro de Investigación Biomédica en Red de Enfermedades Hepáticas y Digestivas (CIBERehd); [‡]Department of Biomedical Sciences, University of Barcelona; [§]Grifols Chair, European Foundation for the Study of Chronic Liver Failure (EF-CLIF), Barcelona, Spain.

Summary sentence: Resolvin D2 modulates the NLRP3 inflammasome and the production of IL-1β in macrophages.

Short running title: Inhibitory actions of SPMs on NLRP3 inflammasome

Corresponding authors: Joan Clària, Hospital Clínic, Villarroel 170, 08036 Barcelona, Spain, E-mail: jclaria@clinic.cat (point of contact)

Aritz Lopategi, IDIBAPS, Rosselló 149-153, 08036 Barcelona, Spain, E-mail: lopategi@clinic.ub.es

Key words: D-series resolvins, inflammation, resolution, innate immune cells

Total character count: 24.568
Total number of figures: 6 Color: 2
Total number of references: 30
Total number of words in abstract: 248
Total number of words in summary sentence: 13

Abbreviations: Absent in melanoma 2 (AIM-2), adenosine tri-phosphate (ATP), apoptosis-associated speck-like protein containing a CARD (ASC), arginase-1 (Arg-1), bone marrow derived macrophages (BMDM), docosahexaenoic acid (DHA), interleukin (IL), lipopolysaccharide (LPS), monocyte chemoattractant protein 1 (MCP-1), nucleotide-binding domain leucine-rich repeat-containing protein 3 (NLRP3), osteopontin (OPN), resolvin D1 (RvD1), resolvin D2 (RvD2), tumor necrosis factor alpha (TNF-α).

ABSTRACT

The prototypic pro-inflammatory cytokine IL-1β plays a central role in innate immunity and inflammatory disorders. The formation of mature IL-1β from an inactive pro-IL-1β precursor is produced via non-conventional multiprotein complexes called the inflammasomes, of which the most common is the NLRP3 inflammasome composed by NLRP3, ASC and caspase-1. Specialized pro-resolving mediators (SPMs) promote resolution of inflammation, which is an essential process to maintain host health. SPMs prevent excessive inflammation by terminating the inflammatory response and returning to tissue homeostasis without immunosupression. This study tested the hypothesis that modulation of the NLRP3 inflammasome in macrophages is one mechanism involved in the SPM-regulated processes during resolution. Our findings demonstrate that the SPM resolvin (Rv) D2 suppressed the expression of pro-IL-1β and reduced the secretion of mature IL-1β in bone marrow-derived macrophages challenged with LPS+ATP (classical NLRP3 inflammasome model) or LPS+palmitate (lipotoxic model). Similar findings were observed in thioglycolate-elicited peritoneal macrophages, in which RvD2 remarkably reduced ASC oligomerization, inflammasome assembly and caspase-1 activity. *In vivo*, in a self-resolving zymosan A-induced peritonitis model, RvD2 blocked the NLRP3 inflammasome leading to reduced release of IL-1β into the exudates, repression of osteopontin and MCP-1 expression and induction of M2 markers of resolution (i.e. CD206 and arginase-1) in peritoneal macrophages. RvD2 inhibitory actions were receptor mediated and were abrogated by a selective GPR18 antagonist. Together, these findings support the hypothesis that SPMs have the ability to inhibit the priming and to expedite the deactivation of the NLRP3 inflammasome in macrophages during the resolution process.

INTRODUCTION

Interleukin (IL)-1β is a potent pro-inflammatory cytokine critical in host defense against infection, presenting pathologically increased levels in inflammatory disorders (1). Unlike many other cytokines, IL-1β is produced via nonconventional multiprotein complexes called the inflammasomes, which are required for the post-translational processing of an inactive 31 kDa precursor, termed pro-IL-1β, into mature IL-1β (2). Inflammasomes also process the maturation of pro-IL-18 into mature IL-18 (2, 3). Several canonical inflammasomes are activated in response to endogenous and exogenous danger signals (2, 3). Each inflammasome is named after its nucleotide-binding domain leucine-rich repeat-containing (NLR) or AIM2-like receptor (ALR), the most common being the NLR protein 3 (NLRP3) inflammasome (2, 3). The NLRP3 inflammasome is assembled when NLRP3 homotypically engages the apoptosis-associated Speck-like protein with a caspase recruitment domain (ASC) to recruit the inactive zymogen pro-caspase-1 (4). Oligomerization of pro-caspase-1 proteins induces their auto-proteolytic cleavage into active caspase-1, a cysteine-dependent protease that cleaves pro-IL-1β and pro-IL-18 to generate the biologically active pro-inflammatory cytokines IL-1β and IL-18, respectively (2-4).

Specialized pro-resolving mediators (SPMs) are potent, local acting lipid mediators endogenously produced from polyunsaturated fatty acid precursors during the inflammation resolution process via a complex coordinated program (5). SPMs are essential to maintain host homeostasis by actively promoting the timely resolution of inflammation exerting their actions at the nanomolar level (5). These bioactive lipid mediators prevent excessive inflammation and the return to tissue homeostasis by limiting leukocyte trafficking and the production of chemical pro-inflammatory mediators such as cytokines, among others (5). The SPM family is composed of different class members, namely resolvins of the E-

series, which are generated from eicosapentaenoic acid, resolvins of the D series generated from docosahexaenoic acid (DHA) and protectins and maresins also derived from DHA (5). Among the SPM family, in the current study we focused our attention on resolvins of the D-series and in particular in resolvin (Rv) D1 and RvD2, which are the most widely characterized and their receptors have been identified and cloned (6,7). In addition, these SPMs potently reduce the secretion of pro-inflammatory cytokines by activated macrophages, and more specifically are capable of reducing the expression of IL-1β at the mRNA level in THP-1 monocytic cells (8), burn wound neutrophils (9) and vascular smooth muscle cells (10) as well as to reduce the levels of mature IL-1β protein in adipose tissue (11), liver (12) and THP-1 macrophages (13). However, the molecular determinants underlying the modulatory actions of these SPMs on IL-1β levels have not yet been characterized. The aim of the current study was to investigate whether RvD1 and RvD2 were able to modulate the NLRP3 inflammasome in macrophages, thus providing a mechanism by which these SPMs reduce IL-1β formation during the resolution of inflammation.

Materials and Methods

Materials

RvD1 (7S,8R,17S-trihydroxy-4Z,9E,11E,13Z,15E,19Z-DHA), RvD2 (7S,16R,17S-trihydroxy-4Z,8E,10Z,12E,14E,19Z-DHA) and the RvD2 receptor (GPR18) antagonist O-1918 were obtained from Cayman Chemicals (Ann Arbor, MI). Sodium palmitate, Dulbecco's Modified Eagle Medium (DMEM), fatty acid-free (FAF) bovine serum albumin (FAF-BSA), Brewer thioglycolate medium, LPS, ATP and zymosan A were from Sigma (St. Louis, MO). FBS and Dulbecco´s PBS with ($DPBS^{++}$) and without ($DPBS^{--}$) calcium and magnesium were from Lonza (Verviers, Belgium). The High-Capacity Archive kit and TaqMan Gene Expression Assays were from Applied Biosystems (Foster City, CA). Protease inhibitor mixture (Complete™Mini) and phosphatase inhibitor mixture (PhosSTOP™) were from Roche Applied Science (Mannheim, Germany). Antibodies against mouse pro-IL-1β and pro-caspase-1 were from Santa Cruz Biotechnology (Santa Cruz, CA). Caspase-GLO® 1 Inflammasome Assay was from Promega (Fitchburg, WI). Raw 264.7 cells were purchased from European Collection of Cell Cultures (ECACC, Salisbury, UK).

Animals and in vivo peritonitis model

Male C57BL/6J mice from Charles River Laboratories (Saint Aubin les Elseuf, France) were housed in wood-chip bedding cages with 50–60% humidity and a 12-h light/dark cycle and given free access to food and water. Murine peritonitis was induced by intraperitoneal (i.p.) administration of zymosan A at 1 mg/mouse, suspended in 1 ml of sterile saline with or without RvD1 or RvD2 (300 ng/mouse). This dose was chosen based on our own preliminary data and other studies from the literature (12,14). At selected time intervals (4, 12 and 24 h), mice were euthanized with isofluorane overdose and peritoneal exudates were collected by lavaging the peritoneum with 7 ml of ice-cold $DPBS^{--}$. To isolate intraperitoneal

macrophages, the exudates were centrifuged at 500 g for 5 min and the pellet resuspended in DMEM supplemented with penicillin (100 U/ml), streptomycin (100 mg/ml), L-glutamine (2 mM) and 5% FBS. Cells ($1.4x10^6$ or $7x10^5$ cells/well seeded on 6- or 12-well culture plates, respectively) were allowed to adhere over 2 h at 37°C in a humidified 5% CO_2 incubator. Non-adherent cells were removed by washing twice with $DPBS^{--}$, and RNA and protein were extracted from the remaining adherent cells. In some experiments, macrophages were left growing in DMEM for 12 h and their ability to produce IL-1β was assessed by ELISA. In another set of experiments, peritoneal exudates were directly processed and labeled for flow cytometry analysis (see below). All animal studies were conducted in accordance with the Investigation and Ethics Committee criteria of the Hospital Clínic and European Union legislation.

Isolation of thioglycolate-recruited peritoneal macrophages

Both resting and thioglycolate-recruited (3 days after i.p. injection of 2.5 ml 3% thioglycolate) peritoneal macrophages from C57BL/6J mice were collected by peritoneal lavage with 7 ml of ice-cold $DPBS^{--}$. The exudates were treated as above. To assess inflammasome activation, resting cells were exposed to vehicle (0.01% ethanol) and LPS (100 ng/ml) for 4 h and then incubated with ATP (1 h) or sodium palmitate (200 μM) (12 h) with or without RvD1 or RvD2 (10 nM). The concentration of RvD1 and RvD2 was selected from the literature, which indicates that SPMs exert biological actions within the nanomolar range at concentrations as low as 1-10 nM (5,15). At the end of the incubation period, medium was collected and macrophages were washed twice with $DPBS^{++}$ and then suspended in TRIzol reagent or RIPA buffer (50 mM Tris-HCl, 1 mM EDTA, 1 mM PMSF, 1% Igepal, 0.25 % sodium deoxycholate, 1 mM sodium fluoride, 1 mM sodium orthovanadate, 150 mM NaCl, pH=8,

with a protease and phosphatase inhibitor mix) for RNA and protein extraction and analysis, respectively.

Isolation of bone marrow-derived macrophages (BMDM)

Mice were anesthetized with isofluorane and sacrificed by cervical dislocation. Bone marrow cells from femurs and tibiae of donor C57BL/6J mice were collected in $DPBS^{--}$. After centrifugation at 500 g, the cells were plated at $1x10^5$ cells/cm^2 in complete DMEM with 30% L929-conditioned medium for macrophage differentiation to BMDM (16). To study inflammasome activation, the cells were treated as above and RNA and protein were collected.

RNA isolation, reverse transcription and g*ene expression profiling by real-time PCR*

Isolation of total RNA from peritoneal macrophages and BMDM was performed using the TRIzol reagent. RNA concentration was assessed in a NanoDrop-1000 spectrophotometer (NanoDrop Technologies, Wilmington, DE) and its integrity tested on a 6000 LabChip in a Bioanalyzer 2100 (Agilent Technologies, Santa Clara, CA). cDNA synthesis from 200 to 400 ng of total RNA was performed using the High-Capacity cDNA Archive Kit. For quantification of gene expression by real-time PCR, validated and predesigned TaqMan Gene expression assays were used [Nlrp3 (ID: Mm00840904_m1), Asc (Pycard) (ID: Mm00445747_g1), caspase-1 (ID: Mm00438023_m1), IL-1β (ID: Mm01336189_m1), IL-6 (ID: Mm00446190_m1), TNF-α (ID: Mm00443258_m1), IL-18 (ID: Mm00434225_m1), arginase-1 (Arg1; ID: Mm00475988_m1), mannose receptor C type 1 (CD206) (Mrc1; ID: 00485148_m1), osteopontin (OPN, Spp1) (ID: Mm00436767_m1), 5-lipoxygenase (5-LOX) (Mm001182743_m1) and 12/15-LOX (ID: Mm00772337_m1) using β-actin (Actb; ID: Mm00607939_s1) as endogenous control]. Real-time PCR amplifications were carried out in

an Applied Biosystems 7900HT Fast Real Time PCR System. PCR results were analyzed with the Sequence Detector Software version 2.1 (Applied Biosystems). Relative quantification of gene expression was performed using the comparative Ct method. The amount of target gene, normalized to β-actin and relative to a calibrator, was determined by the arithmetic equation $2^{-\Delta\Delta Ct}$ described in the comparative Ct method (User Bulletin #2; http://docs.appliedbiosystems.com/pebiodocs/04303859.pdf).

Caspase-1 activity assay

Caspase-1 activity was measured using the Caspase-GLO® 1 Inflammasome Assay following the manufacturer's instructions. Briefly cells were plated in 96-well clear bottom plates and exposed to LPS plus palmitate in the presence or absence of RvD2 and 100 μl of medium was separated to measure caspase-1 activity. Then the caspase-1 luciferase Z-WEHD-aminoluciferin substrate was added and the formation of the luminescent product was monitored in a FLUOstar OPTIMA luminometer (BMG Labtech, Ortenberg, Germany). An inhibitor of caspase-1 activity, Ac-YVAD-CHO, was added in duplicate wells to measure non-specific signal. The results are presented as relative luminescence units (RLU).

ASC speck formation

Thioglycolate-recruited peritoneal macrophages were seeded in 8-well flat-bottom permanox labtechs (120,000 cells/well) and incubated with vehicle, LPS (100 ng/mL) plus PA (200 μM) or LPS-PA plus RvD2 (10 nM). Cells were fixed with 4% paraformaldehyde in PBS for 30 min at 37 ºC, and permeabilized/blocked with 10% goat serum, 1% FBS and 0.5% Triton X-100 containing buffer (perm/block buffer) for 30 min at 37 ºC. Cells were then incubated in perm/block buffer containing 1 μg of anti-ASC antibody (AG-25B-0006, Adipogen, San Diego, CA), washed with perm/block buffer and followed by an incubation with perm/block

buffer containing 2.5 μg/mL of Alexa Fluor 488 antibody (R37116, Thermofisher, Rockford, IL). Finally, cells were again washed with perm/block buffer before incubating with DPBS containing 5 μM of Hoechst 33342 (H3570, Thermofisher) for nuclei staining. Cells were visualized in a TCS SP5 confocal microscope (Leica, Wetzlar, Germany).

Cell Viability Assay

Thioglycolate-recruited peritoneal macrophages were seeded in 96-well plates (120,000 cells/well) and incubated with vehicle (EtOH), RvD1 (1, 10 and 100 nM) or RvD2 (1, 10 and 100 nM) and MTT (3-(4,5-dimethylthiazol-2-yl)-2,5-diphenyltetrazolium bromide) for 4 h at 37°C. The reaction was stopped with isopropyl alcohol and shaking for 20 min and the absorbance at 570 nm of the insoluble formazan measured in a multiwell plate reader (BMG Labtech, Offenburg, Germany) and cell number was calculated from a standard curve.

IL-1β ELISA assay

Cell supernatants were collected and IL-1β levels were evaluated by ELISA using High Absorbance 96-well plates and mouse IL-1β ELISA and TMB substrate sets from Beckton Dickinson (San Diego, CA), following the manufacturer's instructions.

Western blot analysis

Protein samples in RIPA Buffer were quantified with the Micro BCA protein assay kit and subjected to electrophoresis in reducing conditions with 13% (for IL-1β) or 15% (for caspase-1) poly-acrylamide gels using the Bio-Rad Mini-Protean system. The proteins were transferred to PVDF membranes using the iBlot Dry Blotting system from Life Technologies following the manufacturer's instructions. The membranes were blocked for 1 h in 5% BSA-TBS-0.5% Tween-20 and incubated with the appropriate antibodies overnight at 4ºC. After

washing, the membranes were blotted with the appropriate HRP-conjugated secondary antibody and the blots were developed with ECL reagent from Biological Industries (Kibbutz Beit Haemek, Israel) in an ImageQuant LAS 4000 image system and analyzed with the ImageQuant TL 7.0 software, both from GE Healthcare. The intensity of bands was normalized to the corresponding values of β-actin.

Flow Cytometry

For immunophenotyping experiments, isolated peritoneal macrophages were resuspended in basic sorting buffer ($DPBS^{--}$ containing 1 mM EDTA, 25 mM HEPES pH 7, and 1% FBS), counted, filtered through a 35-μm nylon mesh, and prepared for flow cytometry analysis. Briefly, macrophages ($1.25x10^6$ cells/ml) were incubated at 4°C with Mouse BD Fc Block (2.5 mg/ml) prior to staining with fluorescently labeled primary antibodies or isotype controls IgGs for 50 min at 4°C in the dark. Thereafter, cells were fixed and permeabilized (Fix&Perm, Invitrogen, Carlsbad, CA) to label the intracellular IL-1β. The antibodies used in these studies included: CD206-APC (0.625 mg/ml), F4/80–PE (0.5 mg/ml) and IL-1β-DyLight-488 (0.5 mg/ml). After incubation with primary antibodies, cell suspensions were washed in 1 ml basic sorting buffer and centrifuged at 500 g for 5 min. The cells were suspended in 0.5 ml basic sorting buffer and analyzed by flow cytometry with a BD FACSCanto II cytometer and FACSDiva v6.1.3 software (BD Biosciences, San Jose, CA). Propidium iodide (4 μg/ml) was used to exclude dead cells. Unstained, single stains, and fluorescence minus one controls were used for setting compensation and gates.

Statistical analysis

Statistical analysis of the results was performed by analysis of variance (one-way or two-way ANOVA) or unpaired Student's t-test. The results are expressed as mean ± SEM and differences were considered significant at $P < 0.05$.

RESULTS

SPMs attenuate LPS-ATP inflammasome activation in BMDM.

To investigate whether RvD1 and RvD2 can modulate the NLRP3 inflammasome in macrophages, we exposed BMDM to the classical NLRP3 inflammasome activation model with LPS and ATP. As shown in **Figure 1A**, LPS alone induced the expression of pro-caspase-1 and pro-IL-1β at the protein level. The addition of ATP to LPS-treated BMDM resulted in a reduction of pro-IL-1β levels, indicating inflammasome activation and the processing of pro-IL-1β to mature IL-1β **(Figure 1A**). The densitometric analysis of the gel bands corresponding to pro-caspase-1 and pro-IL-1β are shown in **Figures 1B** and **1C**, respectively. Consistent with inflammasome activation, secretion of mature IL-1β protein was increased ≅27-fold after stimulation of BMDM with LPS and ATP **(Figure 1D**). Incubation of LPS-ATP-elicited macrophages with RvD2 significantly reduced pro-IL-1β protein levels and the secretion of the mature form of IL-1β protein (**Figures 1A, 1C** and **1D**). The inhibitory actions of RvD2 on inflammasome processing of mature IL-1β were abrogated by the presence of O-1918, a selective antagonist of GPR18, the recently described RvD2 receptor (7) (**Figure 1E**). Protein levels of pro-caspase-1 were not significantly modified by this SPM (**Figures 1A** and **1B**). Furthermore, both RvD1 and RvD2 potently inhibited the expression of IL-1β at the mRNA level (**Figure 1F**), indicating that these SPMs primarily block the priming of the NLRP3 inflammasome. Consistent with this view, the mRNA expression of IL-18, another inflammatory cytokine which maturation is also processed by the NLRP3 inflammasome, was also down-regulated by RvD1 and RvD2 (**Figure 1G**). The inhibitory actions of these SPMs on inflammasome priming were associated with down-regulation of pro-inflammatory genes such osteopontin (OPN), confirming that the macrophage inflammatory phenotype was toned down by these lipid mediators (**Supplementary Figure**

1A). These effects were not associated with changes in cell viability after treatment with RvD1 or RvD2 at the concentrations used in our *in vitro* studies (**Supplementary Figure 1B**).

SPMs attenuate LPS-palmitate inflammasome activation in BMDM.

To ascertain whether the SPM inhibitory properties were also seen in other models of NLRP3 inflammasome activation, we next challenged BMDM with LPS and palmitate. In these experiments, both RvD1 and RvD2 significantly reduced both palmitate-induced and LPS-palmitate-induced pro-IL-1β protein levels (**Figures 2A** and **2C**). However, only RvD2 treatment resulted into a significantly lower secretion of mature IL-1β to the medium (**Figure 2D**). No changes in pro-caspase-1 levels were observed (**Figure 2B**). Similar to that seen in the LPS-ATP model, the most striking observation was the inhibitory action of RvD1, and especially of RvD2, on IL-1β mRNA expression (**Figure 2E**). IL-18 as well as MCP-1 mRNA levels were also blocked by SPMs in BMDM challenged with LPS and palmitate (**Figures 2F** and **2G**). OPN mRNA expression was also blocked by RvD1 and RvD2 (**Supplementary Figure 1C**). Of interest, RvD1 and RvD2 enhanced the expression of 12/15-LOX, a gate-keeper enzyme of the biosynthesis of lipid mediators of resolution (**Figure 2H**). No changes in 5-LOX were detected (**Figure 2I**).

SPMs attenuate LPS-palmitate inflammasome activation in peritoneal macrophages.

To further confirm the modulatory properties of SPMs on the macrophage NLRP3 inflammasome, we next explored the actions of RvD1 and RvD2 on thioglycolate-recruited peritoneal macrophages. As shown in **Figure 3A** *(left panel),* exposure of peritoneal macrophages to increasing concentrations of LPS (from 0 to 1000 ng/ml) induced the accumulation of the IL-1β precursor pro-IL-1β, while the protein levels of pro-caspase-1 remained unaffected. This induction was also seen in naive Raw 264.7 cells, a murine

macrophage cell line (**Figure 3A,** *right panel*). As expected, the addition of palmitate to LPS-stimulated peritoneal macrophages resulted in the activation of the inflammasome manifested in a significant reduction of the levels of unprocessed pro-IL-1β protein (**Figure 3B**), accompanied by an increase in the secretion of mature IL-1β to the media (**Figure 3C**). Incubation of palmitate-challenged peritoneal macrophages with RvD1 or RvD2 was associated with a significant inhibition in pro-IL-1β protein levels without changes in pro-caspase-1 (**Figure 3D**). Similar to that previously seen in BMDM, both RvD1 and RvD2 produced a striking reduction in IL-1β mRNA expression in LPS-palmitate-challenged macrophages (**Figure 3E**), effects that culminated into a lower secretion of mature IL-1β protein into the media (**Figure 3F**). Caspase-1 mRNA levels in peritoneal macrophages were not greatly affected by SPMs (**Figure 3G**). Of interest, RvD1 and RvD2 did not show additive actions on the LPS-priming of IL-1β expression, suggesting different signalling pathways for their actions (**Supplementary Figure 1D**).

RvD2 inhibits caspase-1 activity in LPS-palmitate-elicited peritoneal macrophages.

Once established that variations in IL-1β in response to SPMs occur in the context of reduced inflammasome priming, we next sought to investigate whether these lipid mediators could also modify caspase-1 activity despite not observing changes in its expression. These experiments were performed with RvD2 because only this SPM showed a consistent inhibition on the secretion of mature IL-1β across the different experimental conditions (see **Figures 1-3**). As shown in **Figure 4A**, RvD2 significantly reduced in a concentration-dependent manner intracellular caspase-1 activity in peritoneal macrophages challenged with LPS and palmitate. Similarly, a reduction in extracellular caspase-1 activity was observed in macrophages exposed to LPS and palmitate and treated with RvD2 (**Figure 4B**). Confirmatory evidence of repression of inflammasome assembly by RvD2 was obtained by

monitoring ASC speck formation by confocal microscopy (**Figure 4C**). RvD1 did not exert any significant effect on caspase-1 activity (**Supplementary Figure 1E**). Caspase-1 inhibition by RvD2 may have broader implications, since apart from the processing and maturation of IL-1β, caspase-1 is also a key player in pyroptosis, a process that fuels the inflammatory response through the massive release of intracellular inflammatory components by dying macrophages (17). Along these lines, in our experiments, flow cytometry analysis revealed a higher number of viable double F4/80-IL-1β positive cells (i.e. macrophages) after RvD2 treatment (**Figure 4D**), confirming that RvD2 did not induce pyroptosis in peritoneal macrophages. This finding was consistent with the observation that RvD2 did not reduce macrophage viability (**Supplementary Figure 1B**).

RvD2 deactivates NLRP3 inflammasome in zymosan A-induced peritonitis.

To translate *in vivo* our *in vitro* findings, we next explored the actions of SPMs in an experimental model of murine peritonitis, which is characterized by spontaneous resolution of inflammation within 24 h after the injection of zymosan A. Preliminary observations indicated that RvD2 was the most active SPM of the resolvin D-series in this model, and therefore this lipid mediator was again selected for *in vivo* studies. Over the course of resolution, the NRLP3 inflammasome was progressively deactivated in peritoneal macrophages resulting in reduced NLRP3 mRNA levels without changes in ASC and caspase-1 (**Figure 5A**). Decreased IL-1β mRNA expression, sustainably lower IL-1β secretion and reduced mature IL-1β levels in the peritoneal exudates were also detected over the resolution process (**Figure 5B**). Although no significant differences were observed in the expression of caspase-1, NLRP3 and ASC**,** as compared to peritoneal macrophages from mice receiving zymosan A alone (**Figure 5C**), macrophages isolated from mice receiving zymosan A and RvD2 exhibited a faster and more pronounced deactivation of the inflammasome

during the resolution process resulting in lower IL-1β mRNA expression and IL-1β protein secretion (**Figures 5D and 5E**). Consistent with this, lower levels of mature IL-1β protein were detected in peritoneal exudates from mice treated with RvD2 (**Figure 5F**).

RvD2 suppresses the inflammatory phenotype while promoting the M2 pro-resolutive phenotype in peritoneal macrophages.

Finally, to prove that inflammasome deactivation by RvD2 *in vivo* has broader suppressive effects on inflammation than just reducing IL-1β levels, we assessed the cytokine profile in the self-resolving model of zymosan A-induced peritonitis. As shown in **Figure 6A**, the process of resolution was associated with down-regulation of inflammatory cytokines including IL-6 and TNF-α in parallel with an induction of pro-resolutive M2 markers such as arginase-1 (Arg1) and mannose receptor CD206. Confirmation of the acquisition of a resolution phenotype was obtained by flow cytometry analysis, which revealed a peak in the number of M2 pro-resolutive ($F4/80^{+}/CD206^{+}$) macrophages at 24 h after zymosan A injection (**Figure 6B**). Notably, as compared to mice receiving zymosan A alone, macrophages from mice receiving zymosan A and RvD2 exhibited a significantly higher population of pro-resolutive ($F4/80^{+}/CD206^{+}$) macrophages at 12 h after zymosan challenge (**Figure 6B**). Consistent with this, at 12 h, RvD2 significantly up-regulated Arg1, which is a functional marker of M2 macrophages (**Figure 6C**). Moreover, at this time period, macrophages from mice receiving zymosan A and RvD2 exhibited an attenuated expression of M1 cytokines such as OPN and TNF-α (**Figure 6D**). Comparison of the different macrophage populations did not identify any difference in cell viability from RvD2-treated versus non-treated animals (**Supplementary Figure 1F** and **Supplementary Figure 2**). Together, these data confirm the dominance of pro-resolving and anti-inflammatory conditions in macrophages from mice receiving the RvD2 treatment.

DISCUSSION

The results of the current study indicate that SPMs are able to modulate IL-1β production in macrophages by inhibiting the priming and repressing the activation of the NLRP3 inflammasome. To reach this conclusion, we employed both *in vitro* and *in vivo* approaches. In particular, we utilized two different *in vitro* models of inflammasome activation (LPS plus ATP (the classical inflammasome activation model) and LPS plus palmitate (the lipotoxic inflammasome activation model)) in macrophages from two different sources (i.e. bone marrow-derived and peritoneal). *In vivo*, we performed experiments in peritoneal macrophages isolated from mice with zymosan A-induced peritonitis, a useful model of self-resolving and limited inflammation. In all these experimental conditions, we obtained data indicating that SPMs of the resolvin D-series inhibit IL-1β expression. Inhibition of IL-1β expression by D-series resolvins was observed at both mRNA and protein levels, although protein changes were more modest, reinforcing the concept that these SPMs preferentially block the priming of the inflammasome. This finding might also be explained by the observation described by Perl et al showing that changes at the mRNA level are sometimes poorly correlated with changes at the protein level, explaining why in some conditions changes at the protein level are attenuated (18). Of note, changes in IL-1β at the mRNA and protein levels were only accompanied by a reduction in the secretion of the mature form of this cytokine when murine macrophages were treated with RvD2. In fact, only RvD2 was able to inhibit caspase-1 activity during inflammasome assembly, the enzyme responsible for the processing of mature IL-1β protein. The inhibitory actions of RvD2 on caspase-1 activity might be secondary to the prevention of ASC oligomerization and inflammasome assembly, since RvD2 reduced ASC speck formation in macrophages. Moreover, inhibition of caspase-1 activity in response to RvD2 also suggests that this SPM might be useful in protecting macrophages from pyroptosis, a form of caspase-1-dependent programmed cell death that

results in the rapid lysis of the cells and the release of inflammatory cytokines such as IL-1β into the extracellular milieu (17).

Although the findings of the current study in murine macrophages are consistent with previous data demonstrating a more potent activity of RvD2 than RvD1 in other tissues and cells (11), the reason why two structurally related lipid mediators such as RvD1 and RvD2 differ in their potency in inhibiting the inflammasome deserves further discussion. It can be speculated that this different activity could be secondary to the fact that these two structurally related resolvins act through two different receptors: RvD1 binds to ALX and GPR32 whereas RvD2 binds to GPR18 (6,7). However, in our study the simultaneous use of RvD1 and RvD2 did not provide an additional benefit as compared to RvD1 or RvD2 alone. On the other hand, the superiority of RvD2 actions on the inflammasome could be related to a major stability of this SPM in the biological milieu. In this regard, RvD2 was demonstrated to be more resistant to local inactivation by 15-prostaglandin-dehydrogenase/eicosanoid oxidoreductase than RvD1, a finding that resulted in a higher stimulatory activity of adiponectin secretion by RvD2 in obese adipose tissue (11). The reason why RvD2 induced a more potent inhibitory action on the LPS plus ATP inflammasome model compared to that of LPS plus palmitate also deserves some discussion. The classical LPS plus ATP model was one of the initial experimental approaches selected to induce the rapid release of large amounts of processed mature IL-1β (19). Extracellular ATP acts as an NLRP3-activating DAMP that is released at sites of cellular injury or necrosis (20). ATP stimulates rapid K^+ efflux from the purinergic ATP-gated ion P2X7 receptor and triggers gradual recruitment and pore formation by the pannexin-1 hemichanel (20). This model of inflammasome activation is therefore representative of conditions in which cell integrity is compromised (i.e. necrosis). In contrast, the LPS plus palmitate is a model representative of lipotoxicity. Palmitate is a

saturated fatty acid that induces the activation of the NLRP3-ASC inflammasome, causing caspase-1-mediated IL-1β production by mechanisms different from those of ATP, in particular through an AMPK-autophagy-ROS signaling pathway (21). Therefore, LPS plus palmitate is a model reproducing lipotoxic conditions encountered in diseases characterized by the presence of increased availability of lipids and other nutrients. For example, this model is useful for investigating the pathophysiology of metabolic associated inflammation leading to insulin resistance and type 2 diabetes.

The findings of the current study are in line with a recent publication suggesting that the NLRP3 inflammasome is a target for DHA-derived metabolites in renal podocytes (22). Our results also concur with findings by Lee et al., who have reported that genetic deficiency of NLRP3 inflammasome protects mice against sepsis via increased formation of lipoxin B_4, an arachidonic acid-derived SPM (23). Furthermore, our findings are consistent with those reported by Dalli et al., who demonstrated that 13-series resolvins (a family of novel bioactive molecules containing conjugated triene and diene double bonds and a 13-carbon position alcohol derived from docosapentaenoic acid (DPA, C22:5)) regulate inflammasome components in human and mouse phagocytes (24). However, some of the findings of the current study are not in agreement with those previously reported by Yan et al. (25). These investigators tested the effects of omega-3 fatty acids on the NLRP3 inflammasome in PMA-differentiated THP-1 macrophages and BMDM and concluded that the ability of these fatty acids to repress the inflammasome is independent of the transformation of omega-3 precursors into bioactive lipid mediators (25). Specifically, these authors provided evidence that neither RvD1 nor aspirin-triggered RvD1 and protectin D1 had any effect on nigericin-induced caspase-1 activation and IL-1β secretion by LPS-primed BMDM (25). Several reasons may account for this discrepancy with our findings. Firstly, Yan et al. used

micromolar concentrations of SPMs, hundred-times higher than those employed in our experiments. The actions of lipid mediators are bell-shaped (26), and the use of such high amounts has a likely negative impact on their biological properties. Secondly, RvD2, which in our study was the most active lipid mediator in inhibiting the priming of inflammasome was not tested by Yan et al. On the other hand, our findings with RvD1 are quite coincidental with theirs because the response to this lipid mediator was also quite modest in our system. Finally, protectin D1 was obtained from commercial sources, and it is widely known that only the protectin D1 isomer called protectin DX, which has no comparable properties, is commercially available (27).

In summary, the present study provides evidence for the ability of SPMs to limit inflammation and expediting resolution by deactivating the NLRP3 inflammasome. The physiological consequences of our results are not limited to the modulation of IL-1β secretion by macrophages but also influence the interpretation of the role of SPMs in the resolution of inflammation. Our findings in the self-resolving model of murine peritonitis support the concept that SPMs facilitate the resolution process by inhibiting the priming and deactivating the inflammasome. This finding is important because IL-1β initiates the inflammatory cascade by activating, among other processes, neutrophil degranulation, expression of adhesion molecules and the release of other cytokines and chemokines, including IL-6, TNF-α and MCP-1, a response that is known as the "cytokine storm" (1,28). Finally, in our studies, SPMs reduced the expression of OPN, a matrix associated protein with potent pro-fibrogenic and pro-inflammatory properties, the overexpression of which delays the resolution of inflammation and fibrosis (29,30).

AUTHORSHIP

Conceived and designed the experiments: A.L. and J.C.; performed the experiments: A.L. and R.F.; provided assistance to experiments and contributed reagents and tools: B.R., C.L-V., J.A-Q, E.T.; wrote the paper: A.L. and J.C.

ACKNOWLEDGEMENTS:

Supported by Spanish MEC (SAF15-63674-R and PIE14/00045) under European Regional Development Funds (ERDF). CIBERehd is funded by the Instituto de Salud Carlos III. This study was carried out at the Center Esther Koplowitz, IDIBAPS, which is part of the CERCA Programme/Generalitat de Catalunya. A.L. was funded by a Marie Curie Action. C.L.-V. was supported by CIBERehd. B.R. had a fellowship from MEC. J.A.-Q. is a recipient of an Agaur/BFU fellowship (FI-DGR 2015). We thank Ana Isabel Martínez-Puchol for her technical assistance.

CONFLICT OF INTEREST DISCLOSURE:

The authors declare no conflict of interest.

REFERENCES

1. Dinarello, C. A. 2009. Interleukin-1beta and the autoinflammatory diseases. *N Engl J Med* 360: 2467-2470.
2. Lamkanfi, M., and V. M. Dixit. 2014. Mechanisms and functions of inflammasomes. *Cell* 157: 1013-1022.
3. Guo, H., J. B. Callaway, and J. P. Ting. 2015. Inflammasomes: mechanism of action, role in disease, and therapeutics. *Nat Med* 21: 677-687.
4. Schroder, K., and J. Tschopp. 2010. The inflammasomes. *Cell* 140: 821-832.
5. Serhan, C. N. 2014. Pro-resolving lipid mediators are leads for resolution physiology. *Nature* 510: 92-101.
6. Krishnamoorthy, S., Recchiuti, A., Chiang, N., Yacoubian, S., Lee, C.H., Yang, R., Petasis, N.A., Serhan, C.N. 2010. Resolvin D1 binds human phagocytes with evidence for proresolving receptors. Proc. Natl. Acad. Sci. USA 107:1660-1665.
7. Chiang, N., J. Dalli, R. A. Colas, and C. N. Serhan. 2015. Identification of resolvin D2 receptor mediating resolution of infections and organ protection. *The Journal of experimental medicine* 212: 1203-1217.
8. Croasdell, A., P. J. Sime, and R. P. Phipps. 2016. Resolvin D2 decreases TLR4 expression to mediate resolution in human monocytes. *FASEB J*. doi:10.358, dot.2016.52.5.2505616
9. Bohr, S., S. J. Patel, D. Sarin, D. Irimia, M. L. Yarmush, and F. Berthiaume. 2013. Resolvin D2 prevents secondary thrombosis and necrosis in a mouse burn wound model. *Wound Repair Regen* 21: 35-43.
10. Kain, V., K. A. Ingle, R. A. Colas, J. Dalli, S. D. Prabhu, C. N. Serhan, M. Joshi, and G. V. Halade. 2015. Resolvin D1 activates the inflammation resolving response at

splenic and ventricular site following myocardial infarction leading to improved ventricular function. *J Mol Cell Cardiol* 84: 24-35.

11. Clària, J., J. Dalli, S. Yacoubian, F. Gao, and C. N. Serhan. 2012. Resolvin D1 and resolvin D2 govern local inflammatory tone in obese fat. *Journal of immunology* 189: 2597-2605.

12. Rius, B., E. Titos, E. Moran-Salvador, C. Lopez-Vicario, V. Garcia-Alonso, A. Gonzalez-Periz, V. Arroyo, and J. Clària. 2014. Resolvin D1 primes the resolution process initiated by calorie restriction in obesity-induced steatohepatitis. *FASEB J* 28: 836-848.

13. Cox, R., Jr., O. Phillips, J. Fukumoto, I. Fukumoto, P. Tamarapu Parthasarathy, M. Mandry, Y. Cho, R. Lockey, and N. Kolliputi. 2015. Resolvins Decrease Oxidative Stress Mediated Macrophage and Epithelial Cell Interaction through Decreased Cytokine Secretion. *PLoS One* 10: e0136755.

14. Sun, Y.P., Oh, S.F., Uddin, J., Yang, R., Gotlinger, K., Campbell, E., Colgan, S.P., Petasis, N.A., Serhan, C.N. 2007. Resolvin D1 and its aspirin-triggered 17R epimer stereochemical assignments, anti-inflammatory properties, and enzymatic inactivation. J Biol Chem. 282: 9323-9334.

15. Clària, J., López-Vicario, C., Rius, B., Titos, E. 2017. Pro-resolving actions of SPM in adipose tissue biology. Mol Aspects Med. 58:83-92.

16. Tomida, M., Y. Yamamoto-Yamaguchi, and M. Hozumi. 1984. Purification of a factor inducing differentiation of mouse myeloid leukemic M1 cells from conditioned medium of mouse fibroblast L929 cells. *The Journal of biological chemistry* 259: 10978-10982.

17. Fink, S. L., and B. T. Cookson. 2005. Apoptosis, pyroptosis, and necrosis: mechanistic description of dead and dying eukaryotic cells. *Infection and immunity* 73: 1907-1916.

18. Perl, K., Ushakov, K., Pozniak, Y., Yizhar-Barnea, O., Bhonker, Y., Shivatzki, S., Geiger, T., Avraham, K.B., Shamir, R. 2017. Reduced changes in protein compared to mRNA levels across non-proliferating tissues. *BMC Genomics* 18:305

19. Kahlenberg, J. M., and G. R. Dubyak. 2004. Mechanisms of caspase-1 activation by P2X7 receptor-mediated K+ release. *American journal of physiology. Cell physiology* 286: C1100-1108.

20. Schroder, K., R. Zhou, and J. Tschopp. 2010. The NLRP3 inflammasome: a sensor for metabolic danger? *Science* 327: 296-300.

21. Wen, H., D. Gris, Y. Lei, S. Jha, L. Zhang, M. T. Huang, W. J. Brickey, and J. P. Ting. 2011. Fatty acid-induced NLRP3-ASC inflammasome activation interferes with insulin signaling. *Nat Immunol* 12: 408-415.

22. Li G, Chen Z, Bhat OM, Zhang Q, Abais-Battad JM, Conley SM, Ritter JK, Li PL. 2017. NLRP3 Inflammasome as a Novel Target for Docosahexaenoic Acid Metabolites to Abrogate Glomerular Injury. J Lipid Res. doi: 10.1194/jlr.M072587.

23. Lee S, Nakahira K, Dalli J, Siempos II, Norris PC, Colas RA, Moon JS, Shinohara M, Hisata S, Howrylak JA, Suh GY, Ryter SW, Serhan CN, Choi AM. 2017. NLRP3 Inflammasome Deficiency Protects Against Microbial Sepsis via Increased Lipoxin B4 Synthesis. Am J Respir Crit Care Med. 196:713-726.

24. Dalli, J., Chiang, N., Serhan, C.N. 2015. Elucidation of novel 13-series resolvins that increase with atorvastatin and clear infections. Nat Med. 21: 1071-5.

25. Yan, Y., W. Jiang, T. Spinetti, A. Tardivel, R. Castillo, C. Bourquin, G. Guarda, Z. Tian, J. Tschopp, and R. Zhou. 2013. Omega-3 fatty acids prevent inflammation and metabolic disorder through inhibition of NLRP3 inflammasome activation. *Immunity* 38: 1154-1163.

26. Shimizu, T. 2009. Lipid mediators in health and disease: enzymes and receptors as therapeutic targets for the regulation of immunity and inflammation. *Annual review of pharmacology and toxicology* 49: 123-150.

27. Balas, L., M. Guichardant, T. Durand, and M. Lagarde. 2014. Confusion between protectin D1 (PD1) and its isomer protectin DX (PDX). An overview on the dihydroxy-docosatrienes described to date. *Biochimie* 99: 1-7.

28. Dinarello, C. A. 1996. Biologic basis for interleukin-1 in disease. *Blood* 87: 2095-2147.

29. Leung, T. M., X. Wang, N. Kitamura, M. I. Fiel, and N. Nieto. 2013. Osteopontin delays resolution of liver fibrosis. *Lab Invest* 93: 1082-1089.

30. Urtasun, R., A. Lopategi, J. George, T. M. Leung, Y. Lu, X. Wang, X. Ge, M. I. Fiel, and N. Nieto. 2012. Osteopontin, an oxidant stress sensitive cytokine, up-regulates collagen-I via integrin alpha(V)beta(3) engagement and PI3K/pAkt/NFkappaB signaling. *Hepatology* 55: 594-608.

FIGURE LEGENDS

FIGURE 1. The specialized pro-resolving mediators (SPMs) resolvin (Rv) D1 and RvD2 attenuate LPS-ATP inflammasome activation in bone marrow-derived macrophages (BMDM). (**A**) Representative western blot analysis of pro-caspase-1 and pro-IL-1β in BMDM exposed to LPS (100 ng/ml) for 4 hours before treatment for 40 min with ATP (5 mM), the classical inflammasome activation model, with the appropriate vehicle (V) and with the presence or absence of RvD1 or RvD2 (10 nM each). (**B, C)** Densitometric analysis of blot intensities for pro-caspase-1 and pro-IL-1β. (**D)** Amount of IL-1β secreted by BMDM as determined by ELISA. (**E**) Levels of secreted IL-1β induced by LPS-ATP in BMDM incubated with RvD2 in the presence or absence of its receptor antagonist O-1918. (**F**) mRNA expression by qPCR of IL-1β in BMDM exposed to the classical inflammasome activation model with LPS and ATP. (**G**) mRNA expression of IL-18 in macrophages exposed to LPS and ATP. Results are expressed as mean+SEM and are pooled from n=3 experiments that were run in duplicate. *, $P<0.05$ versus V; $^{\#}$, $P<0.05$ versus LPS-ATP.

FIGURE 2. The SPMs RvD1 and RvD2 attenuate LPS-palmitate (PA) inflammasome activation in BMDM. (A) Representative western blot of BMDM exposed to LPS (100 ng/ml) plus PA (200 μM) (lipotoxic inflammasome model) and incubated with RvD1 or RvD2 (10 nM each). (**B, C**) Densitometric analysis of blot intensities for pro-caspase-1 and pro-IL-1β. (**D**) Measurement of IL-1β secretion by ELISA in the supernatants of LPS plus PA treated BMDM in the presence or absence of RvD1 or RvD2. (**E**) mRNA expression by qPCR of IL-1β in BMDM exposed to the lipotoxic inflammasome activation model in the presence or absence of RvD1 or RvD2. (**F**) IL-18 mRNA expression in macrophages activated with LPS and PA. (**G**) MCP-1 mRNA expression. (**H**) 12/15-LOX mRNA expression. (**I**) 5-LOX mRNA expression. Results are expressed as mean+SEM and are pooled from n=3

experiments that were run in duplicate. *, P<0.05 versus V; $^{\#}$, P<0.05 and $^{\#\#}$, P<0.01 versus LPS-PA.

FIGURE 3. RvD1 and RvD2 attenuate LPS-PA inflammasome activation in peritoneal macrophages. (**A**) Western blot analysis of peritoneal (*left panel*) and Raw 264.7 (*right panel*) macrophages, exposed to increasing LPS concentrations (0 to 1000 ng/ml). (**B**) Peritoneal macrophages challenged with PA (200 μM), LPS (100 ng/ml) or both. Blot intensities quantification is shown below in bars. (**C**) Detection by ELISA of IL-1β secretion by peritoneal macrophages treated with PA (200 μM), LPS (100 ng/ml) or both. (**D**) Representative Western blot of pro-caspase-1 and pro-IL-1β in peritoneal macrophages treated with PA (200 μM), LPS (100 ng/ml) or both, in the presence or absence of RvD1 (10 nM) or RvD2 (10 nM). (**E**) mRNA expression by qPCR of IL-1β in peritoneal macrophages treated with PA (200 μM) for 16 h after LPS (100 ng/ml) challenge for 4 h, in the presence or absence of RvD1 (10 nM) or RvD2 (10 nM). (**F**) Fold induction in IL-1β secretion by peritoneal macrophages exposed to the lipotoxic inflammasome activation model and treated or not with RvD1 or RvD2. (**G**) mRNA expression by qPCR of pro-caspase-1 in peritoneal macrophages treated as described above. Results are expressed as mean+SEM and are pooled from n=3 experiments that were run in duplicate. *, P<0.05 versus V; $^{\#}$, P<0.05 and $^{\#\#}$, P<0.01 versus LPS-PA.

FIGURE 4. RvD2 inhibits caspase-1 activity in peritoneal macrophages exposed to the lipotoxic inflammasome activation model. (**A**) Luminescence assay of intracellular caspase-1 activity in peritoneal macrophages. Before measurement of caspase-1 activity, the cells were primed with LPS (100 ng/ml) for 4 h and treated with PA (200 μM) for 16 h in the presence or absence of increasing concentrations of RvD2. (**B**) Luminescence assay of

extracellular caspase-1 activity in medium secreted by peritoneal macrophages. Before measurement of caspase-1 activity, the cells were primed with LPS (100 ng/ml) for 4 h and treated with PA (200 μM) for 16 h in the presence or absence of RvD2 (10 or 50 nM). (**C**) ASC speck formation in thioglycolate-recruited peritoneal macrophages primed with LPS and treated with RvD2 before stimulation with PA. Representative photomicrographs (600x magnification). Green: ASC protein; blue: Hoechst-stained nuclei. The white arrows show ASC specks. (**D**) Flow cytometry analysis of the percentage (%) of macrophages (F4/80) with positive intracellular IL-1β signal isolated from mice with zymosan A-induced peritonitis with and without RvD2 (300 ng/mouse) treatment. Results are expressed as mean+SEM and are pooled from n=3 experiments that were run by duplicate. P values are for RvD2 treated versus untreated.

FIGURE 5. RvD2 deactivates the NLRP3 inflammasome during zymosan A-induced murine peritonitis. (**A**) mRNA expression of NLRP3 inflammasome components in peritoneal macrophages isolated after 4, 12 and 24 h of zymosan A (1 mg/mouse) challenge. (**B**) IL-1β expression in peritoneal macrophages (left), IL-1β secreted to the medium (middle) and IL-1β levels in the peritoneal exudate after 4, 12 and 24 h of zymosan A challenge. (**C**) mRNA expression of NLRP3 inflammasome components in peritoneal macrophages isolated after 4, 12 and 24 h of zymosan A (1 mg/mouse) challenge with or without RvD2 (300 ng/mouse). (**D**) IL-1β expression in peritoneal macrophages isolated after 4, 12 and 24 h of zymosan A challenge with or without RvD2 (300 ng/mouse). (**E**) IL-1β secreted to the medium in conditions described in D. (**F**) IL-1β content in the peritoneal exudate during the course of peritonitis. Results are expressed as mean+SEM and are pooled from at least n=3 experiments that were run by duplicate. P values are for 12 and 24 h versus 4h or for RvD2 treated versus untreated.

FIGURE 6. RvD2 suppresses the inflammatory environment and increases macrophage M2 pro-resolutive phenotype. (**A**) mRNA expression of inflammatory cytokines (i.e. IL-6 and TNF-α) and M2 pro-resolutive markers (i.e. Arg1 and CD206) in peritoneal macrophages isolated during the course of peritonitis at 4, 12 and 24 h after zymosan A (1 mg/mouse) treatment. (**B**) Flow cytometry analysis of the evolution of the M2 macrophage population ($CD206^+/F4/80^+$) at 4, 12 and 24 h after zymosan A challenge in the absence or presence of RvD2. Representative FACS plots of $CD206^+/F4/80^+$ macrophages during the course of resolution are shown on the left. (**C**) Expression of the M2 marker Arg1 in peritoneal macrophages after 4, 12 or 24 hours of zymosan A (1 mg/ml) treatment, in the presence or absence of RvD2 (300 ng/mouse). (**D**) OPN and TNF-α expression in peritoneal macrophages after 4, 12 or 24 hours of zymosan A (1 mg/ml) treatment, in the presence or absence of RvD2 (300 ng/mouse). Results are expressed as mean+SEM and are pooled from at least n=3 experiments that were run by duplicate. P values are for 12 and 24 h versus 4 h or for RvD2 treated versus untreated.

Figure 1

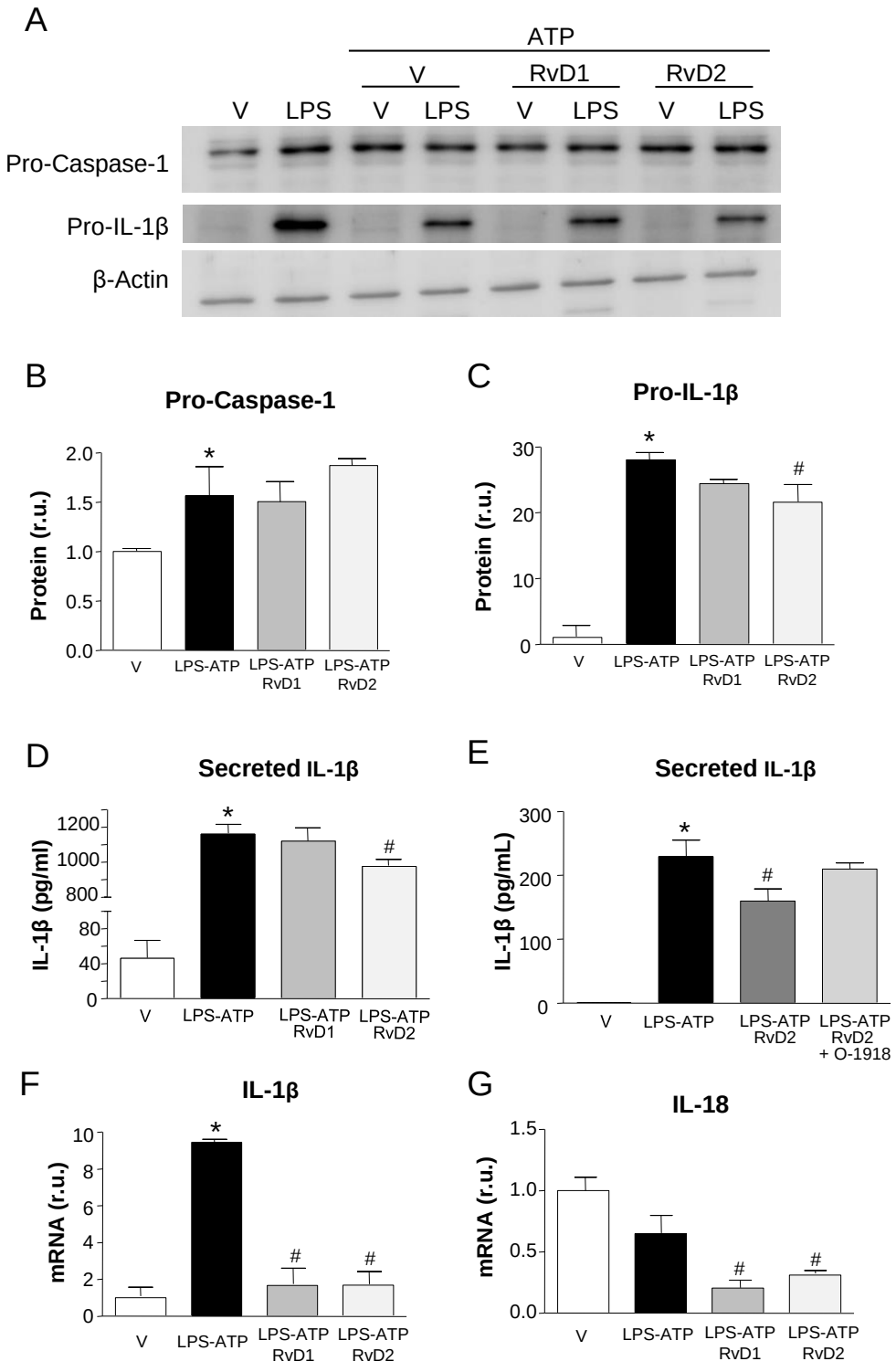
A
ATP
V
RvD1
RvD2
V LPS V LPS V LPS V LPS
Pro-Caspase-1
Pro-IL-1β
β-Actin
B
Pro-Caspase-1
Protein (r.u.)
2.0
1.5
1.0
0.5
0.0
V
LPS-ATP
LPS-ATP RvD1
LPS-ATP RvD2
C
Pro-IL-1β
Protein (r.u.)
30
20
10
0
D
Secreted IL-1β
IL-1β (pg/ml)
1200
1000
800
80
40
0
E
Secreted IL-1β
IL-1β (pg/mL)
300
200
100
0
LPS-ATP RvD2 + O-1918
F
IL-1β
mRNA (r.u.)
10
8
6
4
2
0
G
IL-18
mRNA (r.u.)
1.5
1.0
0.5
0.0

Figure 2

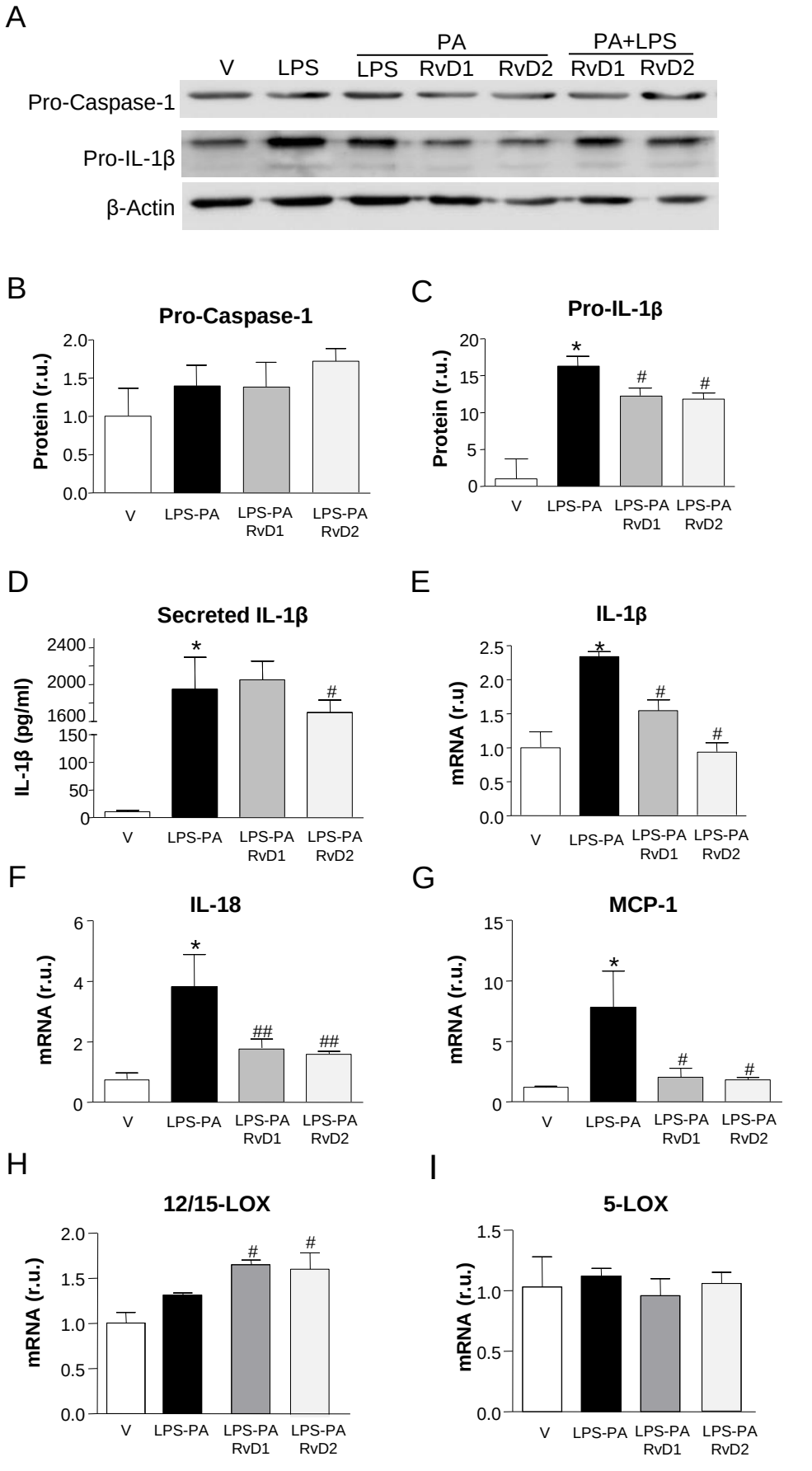
A
V
LPS
PA
LPS
RvD1
RvD2
PA+LPS
RvD1
RvD2
Pro-Caspase-1
Pro-IL-1β
β-Actin
B
Pro-Caspase-1
Protein (r.u.)
2.0
1.5
1.0
0.5
0.0
V
LPS-PA
LPS-PA RvD1
LPS-PA RvD2
C
Pro-IL-1β
Protein (r.u.)
20
15
10
5
0
*
#
#
V
LPS-PA
LPS-PA RvD1
LPS-PA RvD2
D
Secreted IL-1β
IL-1β (pg/ml)
2400
2000
1600
150
100
50
0
*
#
V
LPS-PA
LPS-PA RvD1
LPS-PA RvD2
E
IL-1β
mRNA (r.u)
2.5
2.0
1.5
1.0
0.5
0.0
*
#
#
V
LPS-PA
LPS-PA RvD1
LPS-PA RvD2
F
IL-18
mRNA (r.u.)
6
4
2
0
*
##
##
V
LPS-PA
LPS-PA RvD1
LPS-PA RvD2
G
MCP-1
mRNA (r.u.)
15
10
5
0
*
#
#
V
LPS-PA
LPS-PA RvD1
LPS-PA RvD2
H
12/15-LOX
mRNA (r.u.)
2.0
1.5
1.0
0.5
0.0
#
#
V
LPS-PA
LPS-PA RvD1
LPS-PA RvD2
I
5-LOX
mRNA (r.u.)
1.5
1.0
0.5
0.0
V
LPS-PA
LPS-PA RvD1
LPS-PA RvD2

Figure 3

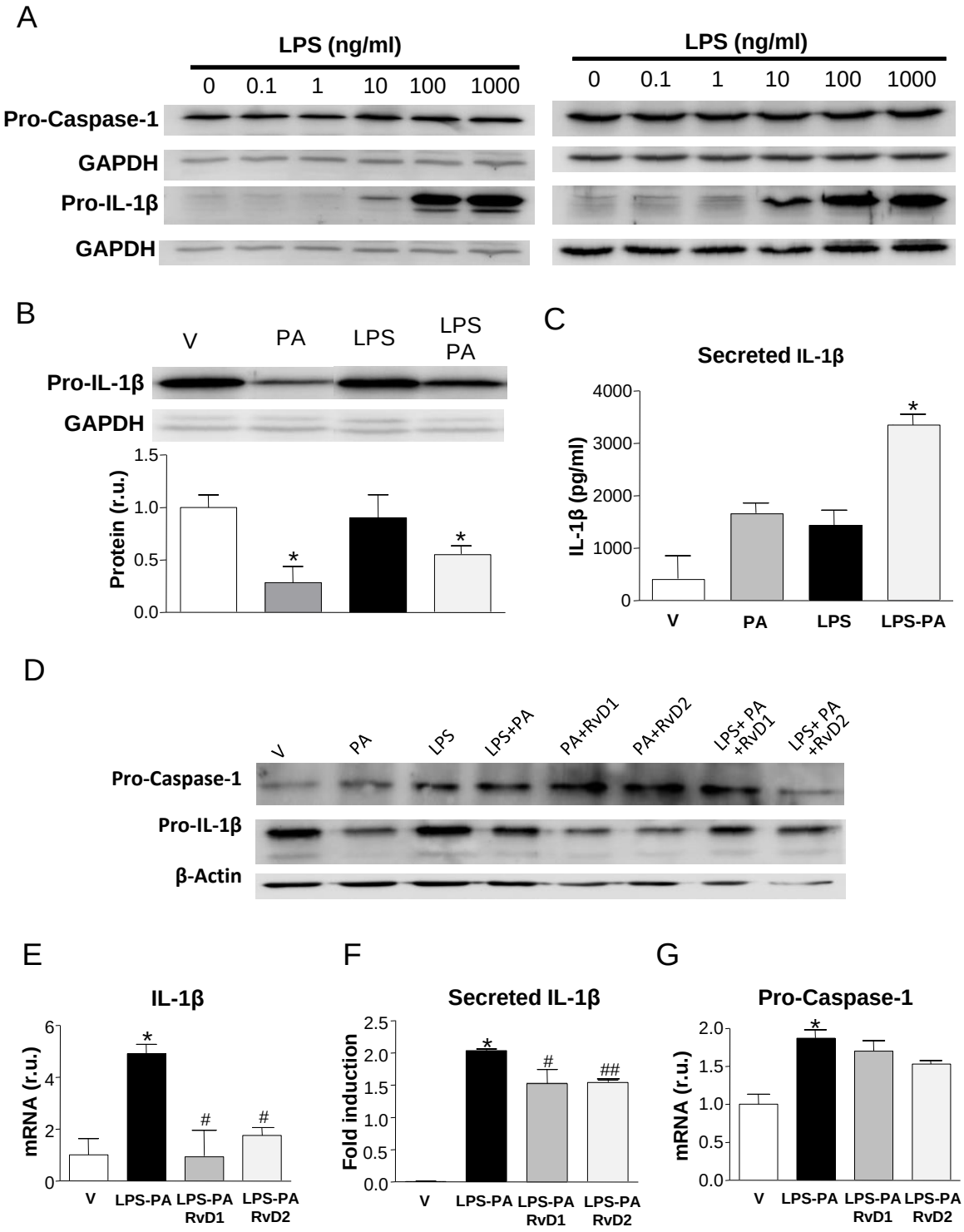
A
LPS (ng/ml)
0 0.1 1 10 100 1000
Pro-Caspase-1
GAPDH
Pro-IL-1β
GAPDH
LPS (ng/ml)
0 0.1 1 10 100 1000
B
V PA LPS LPS PA
Pro-IL-1β
GAPDH
Protein (r.u.)
1.5
1.0
0.5
0.0
C
Secreted IL-1β
IL-1β (pg/ml)
4000
3000
2000
1000
0
V PA LPS LPS-PA
D
V PA LPS LPS+PA PA+RvD1 PA+RvD2 LPS+ PA +RvD1 LPS+ PA +RvD2
Pro-Caspase-1
Pro-IL-1β
β-Actin
E
IL-1β
mRNA (r.u.)
6
4
2
0
V LPS-PA LPS-PA RvD1 LPS-PA RvD2
F
Secreted IL-1β
Fold induction
2.5
2.0
1.5
1.0
0.5
0.0
V LPS-PA LPS-PA RvD1 LPS-PA RvD2
G
Pro-Caspase-1
mRNA (r.u.)
2.0
1.5
1.0
0.5
0.0
V LPS-PA LPS-PA RvD1 LPS-PA RvD2

Figure 4

A

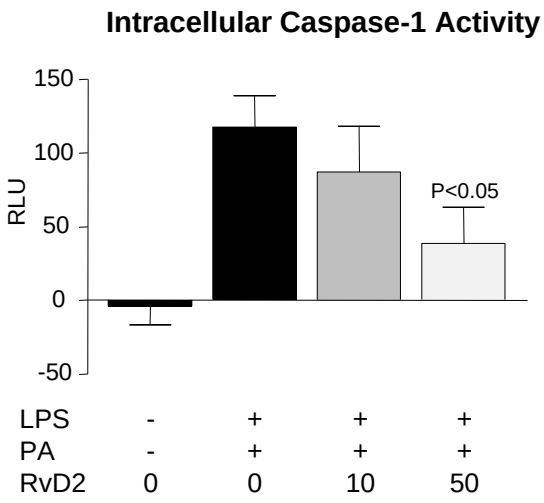

B

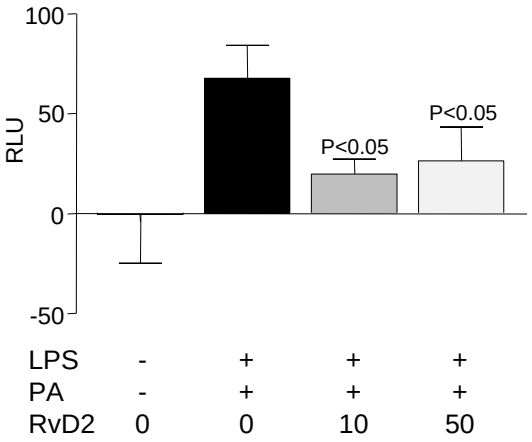

C

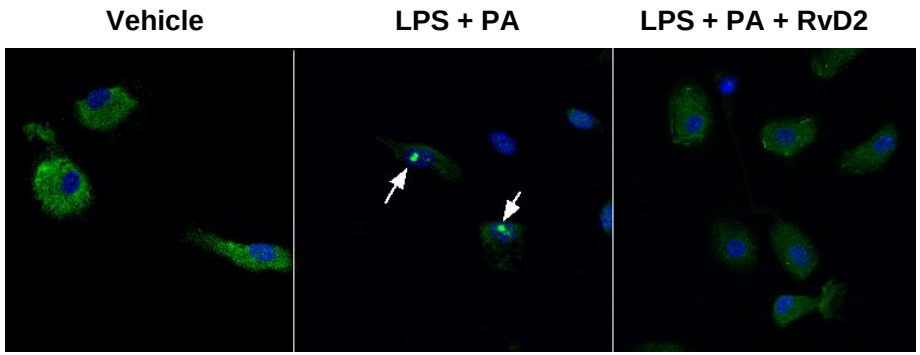

D

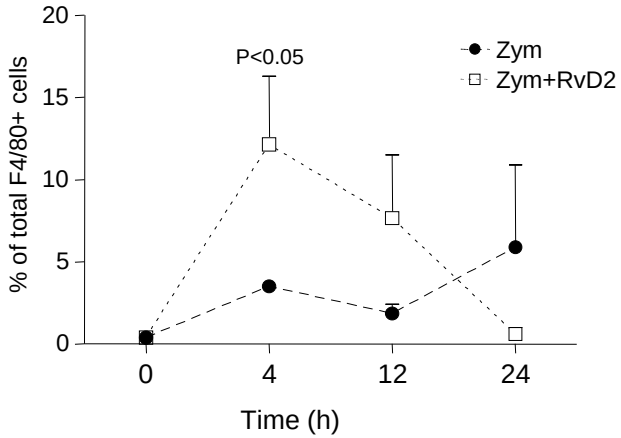

Figure 5

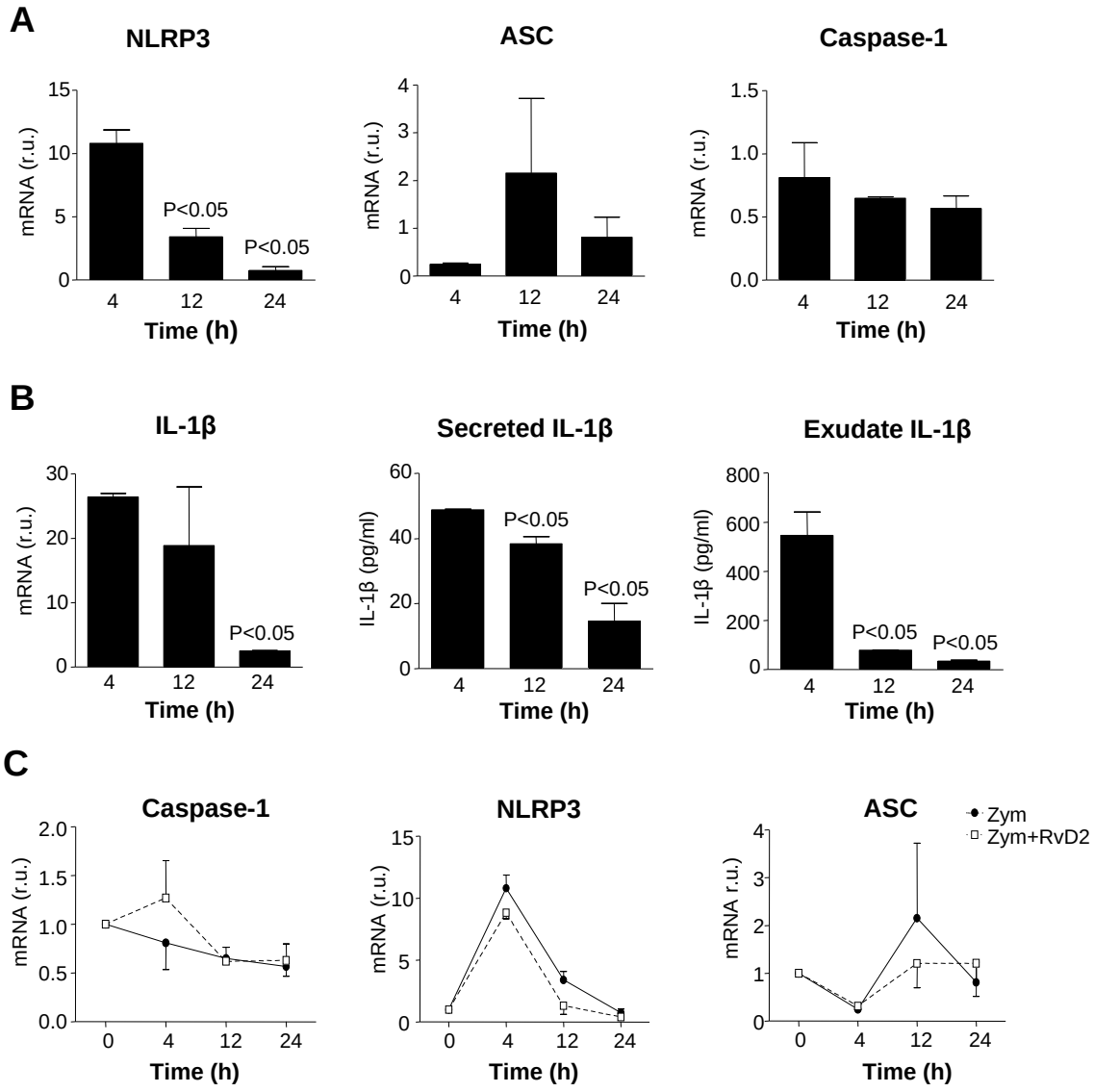
A
NLRP3
ASC
Caspase-1
mRNA (r.u.)
P<0.05
P<0.05
Time (h)
B
IL-1β
Secreted IL-1β
Exudate IL-1β
IL-1β (pg/ml)
C
Caspase-1
NLRP3
ASC
mRNA r.u.
Zym
Zym+RvD2
D
IL-1β
E
Secreted IL-1β
pg/ml
F
Exudate IL-1β
V
D2
4h
12h
24h

Figure 6

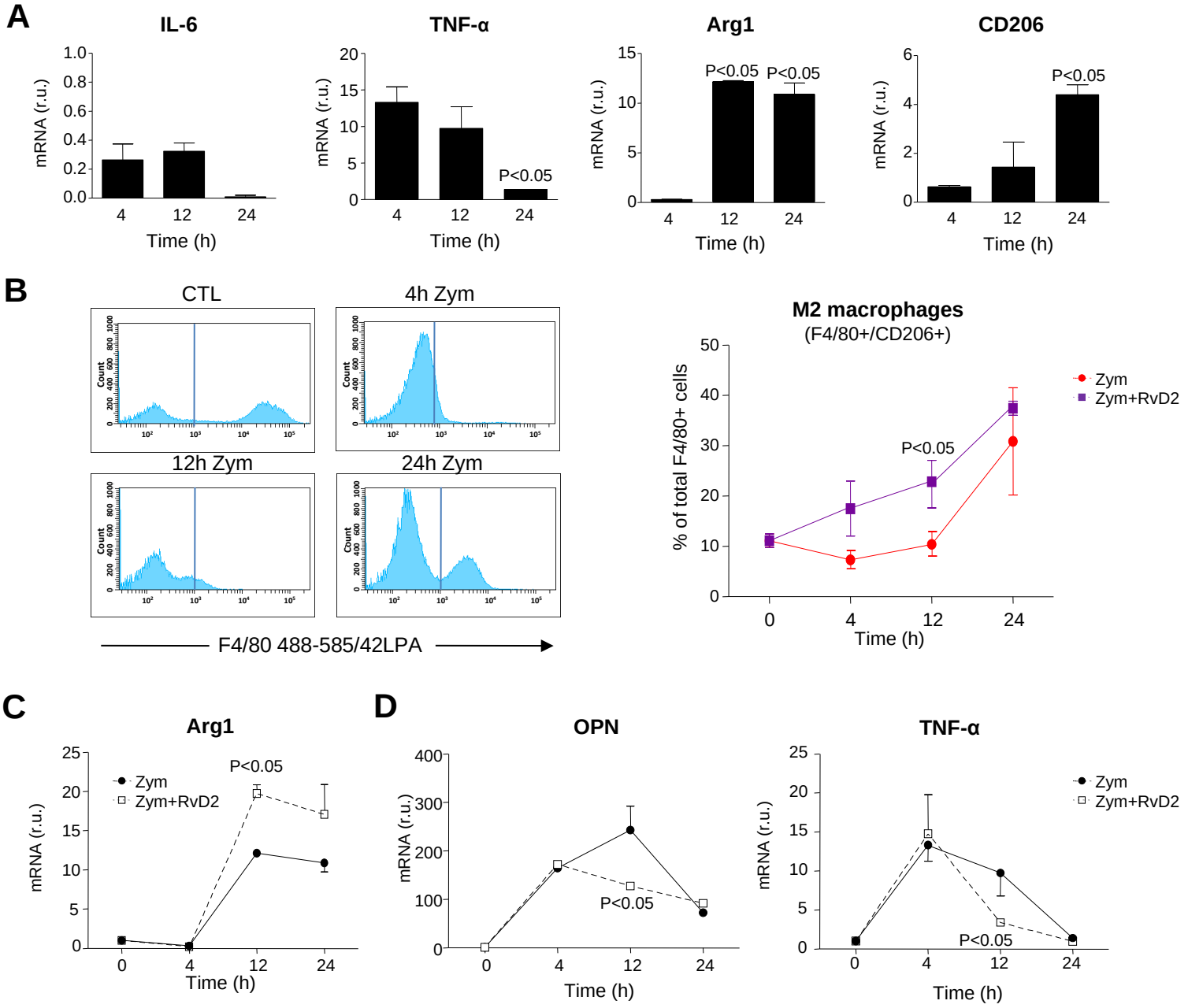
A
IL-6
TNF-α
Arg1
CD206
mRNA (r.u.)
Time (h)
P<0.05
B
CTL
4h Zym
12h Zym
24h Zym
Count
F4/80 488-585/42LPA
M2 macrophages
(F4/80+/CD206+)
% of total F4/80+ cells
Zym
Zym+RvD2
C
Arg1
D
OPN
TNF-α